COMPUTATIONAL MECHANICS
WCCM VI in conjunction with APCOM'04, *Sept. 5-10, 2004, Beijing, China*

Fracture Analysis of Mode III Problems by Trefftz Finite Element Approach

Y. H. Cui[1*], Q. H. Qin[2]

[1] *Department of Mechanics, Tianjin University, Tianjin, 300072, China*
[2] *Department of Engineering, Australian National University, Canberra, ACT 0200, Australia*
email: springc@public.tpt.tj.cn, qinghua.qin@anu.edu.au

Abstract In the present paper, applications of Trefftz finite element method to Mode III problems is presented by way of special purpose functions, auxiliary functions, and a modified variational principle. Trial functions for interpolating intraelement stresses and displacements are introduced and used to derive Trefftz finite element formulation of Mode III problems. In particular, a special purpose element model is presented to represent those elements containing a crack, which can satisfy accurately the fracture behavior of element on crack faces and at crack tips. Furthermore, auxiliary functions are adopted near crack tips to improve computing accuracy. The performance of the proposed element formulation is assessed by an example of a rectangular plate with a side mode III crack, and comparison is made with those obtained by conventional finite element model or by other approaches. The effect of special T-complete system on fracture behavior is also examined.

Key words: fracture analysis, mode III problem, Trefftz finite element approach, auxiliary function

INTRODUCTION

During the past decades the hybrid-Trefftz (HT) finite element method (FEM), originating about twenty five years ago [1], has been considerably improved and has now become a highly efficient computational tool for the solution of complex boundary value problems. Up to now, T-elements have been successfully applied to problems of elasticity [2,3], Kirchhoff plates [4,5], moderately thick Reissner-Mindlin plates [6-8], thick plates [9], general 3-D solid mechanics [10,11], axisymmetric solid mechanics [12], potential problems [13,14], shells [15], elastodynamic problems [16-18], transient heat conduction analysis [19], geometrically nonlinear plates [20-23] and materially nonlinear elasticity [24,25]. Further, the concept of special purpose functions has been found to be of great efficiency in dealing with various geometry or load-dependent singularities and local effects (e.g., obtuse or reentrant corners, cracks, circular or elliptic holes, concentrated or patch loads) [2-4,26,27].
Planar crack problems has been examined by Sabino et al[28] using Trefftz boundary element method and by Freitas and Ji[29] using equilibrium element model. In the present paper, we confine our attention to applications of Trefftz finite element method on Mode III elastic fracture problems. Special T-functions that satisfy free-traction condition along crack faces are used as trial functions for those elements containing a crack. Element matrix equation is deduced by modified variational principles and stress intensity factors are also defined in terms of special functions for mode III crack problem. Numerical results of a rectangular plate with a side mode III crack obtained by the Trefftz finite element method are compared with those obtained by other approaches.

BASIC FORMULATIONS FOR MODE III ELASTIC PROBLEM

1. Governing equation and Boundary conditions In the case of anti-plane shear deformation of isotropic solid, displacements paralleling in the *x-y* plane become zero, i.e., $u=0$ and $v=0$, and in the z direction

$w=w(x,y)\neq 0$, where w is the function of x and y only. Hence, with regards to anti-plane shear deformation or Mode III problem when involving cracks, the differential governing equation can be written as

$$G\left(\frac{\partial^2 w}{\partial x_1^2}+\frac{\partial^2 w}{\partial x_2^2}\right)=0 \qquad \text{in } \Omega \tag{1}$$

and the boundary conditions are

$$w=\overline{w} \qquad \text{on } \Gamma_w \tag{2}$$

$$G\frac{\partial w}{\partial n}=\bar{t} \qquad \text{on } \Gamma_t \tag{3}$$

where G is the shear modulus, w out-of-plane displacement, $\partial w/\partial n$ the normal derivative of w, an overhead bar denotes prescribed value, $\Gamma=\Gamma_w+\Gamma_t$ is the boundary of the solution domain Ω.
The non-zero stress components are given in terms of displacement w as

$$\sigma_{31}=G\frac{\partial w}{\partial x_1}, \quad \sigma_{32}=G\frac{\partial w}{\partial x_2} \tag{4}$$

2. Trefftz functions for Laplace equation It is well-known that the solutions of Eqn (1), the so-called Laplace equation, may be found by using the method of variable separation. By way of this method, the Trefftz functions are obtained as[14]:

$$w(r,\theta)=\sum_{m=0}^{\infty} r^m(a_m\cos m\theta+b_m\sin m\theta) \tag{5}$$

for a bounded region and

$$w(r,\theta)=a_0^*+a_0\ln r+\sum_{m=1}^{\infty} r^{-m}(a_m\cos m\theta+b_m\sin m\theta) \tag{6}$$

for an unbounded region, where r and θ are a pair of polar coordinates. Thus, the associated T-complete sets of Eqns (5) and (6) can be expressed in the form

$$T=\{1, r^m\cos m\theta, r^m\sin m\theta\}=\{T_i\} \tag{7}$$

$$T=\{1, \ln r, r^{-m}\cos m\theta, r^{-m}\sin m\theta\}=\{T_i\} \tag{8}$$

3. Assumed element displacement fields of Trefftz functions To perform finite element analysis, the solution domain Ω is divided into element and each element "e', two independent fields are assumed in the following way:

1) The non-conforming intra-element field The non-conforming intra-element field is expressed by

$$w_e=\breve{w}_e+\sum_{i=1}^{m}\mathbf{N}_{ei}\mathbf{c}_{ei}=\breve{w}_e+\mathbf{N}_e\mathbf{c}_e \tag{9}$$

where $\mathbf{c}_e$ is a vector of undetermined coefficients, m is the number on components[16], and $\breve{w}_e$ and N_{ej} are, respectively, particular and homogeneous solutions to Eqn (1). For any right-hand side $\bar{b}$ ($\bar{b}=0$ in Eqn(1)), $\breve{w}_e$ can be obtained by integration of the source (or Green's) function:

$$w^*(r_{PQ})=\frac{1}{2G\pi}\ln\left(\frac{1}{r_{PQ}}\right) \tag{10}$$

where P designates the field point under consideration, Q stands for the source point (see Fig. 1), and

$$r_{PQ}=\sqrt{(x_{1Q}-x_{1P})^2+(x_{2Q}-x_{2P})^2} \tag{11}$$

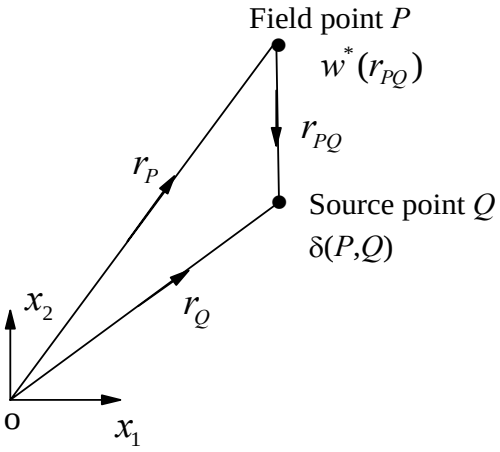

Fig. 1 Notation for Definition of P and Q Points

2) An auxiliary conforming field

$$\tilde{w}_e = \tilde{\mathbf{N}}\mathbf{d}_e \tag{12}$$

is independently assumed along the element boundary in terms of nodal DOF $\mathbf{d}_e$, where $\tilde{\mathbf{N}}$ represents the conventional finite element interpolating functions. For example, a simple interpolation of the frame potential on the side 1-C-2 of a particular element (Fig. 2), the frame functions are defined as

$$\tilde{w}_{12} = \tilde{N}_1 w_1 + \tilde{N}_2 w_2 + \sum_{J=1}^{M} \xi^{J-1}(1-\xi^2) w_{CJ} \tag{13a}$$

where w_{CJ} is shown in Fig. 2,

$$\tilde{N}_1 = \frac{(1-\xi)}{2},\ \tilde{N}_2 = \frac{(1+\xi)}{2}, \tag{13b}$$

and the subscript 'e' for $\tilde{w}_{12}$, w_1 and w_2 has been dropped for simplicity. Hereafter, to further simplify the writing, we shall omit the subscript 'e' in related expressions when the distinction is unnecessary.

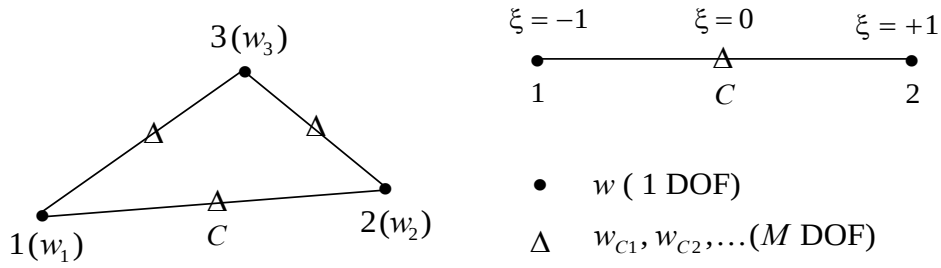

Fig. 2 Geometry of a triangular element

4. Special element containing crack tip In this section we show how special purpose functions can be constructed to satisfy both Eqn (1) and the free-traction boundary conditions on crack faces. The derivation of such functions is based on the general solution of the two-dimensional Laplace equation:

$$w(r,\theta) = a_0 + \sum_{n=1}^{\infty}(a_n r^{\lambda_n} + b_n r^{-\lambda_n})\cos(\lambda_n\theta) + \sum_{n=1}^{\infty}(d_n r^{\lambda_n} + e_n r^{-\lambda_n})\sin(\lambda_n\theta) \tag{14}$$

Appropriate trial functions for a singular corner element are obtained by considering an infinite wedge (Fig. 3) with particular boundary conditions prescribed along the sides $\theta=\pm\theta_0$ forming the angular corner. The boundary conditions for the wedge are

$$\frac{\partial w}{\partial \theta} = 0 \quad (\text{for } \theta = \pm\theta_0) \tag{15}$$

To solve this problem, we rewrite the general solution (14) as

$$w(r,\theta) = a_0 + \sum_{n=1}^{\infty}(a_n r^{\lambda_n} + b_n r^{-\lambda_n})\cos(\lambda_n\theta) + \sum_{n=1}^{\infty}(d_n r^{\beta_n} + e_n r^{-\beta_n})\sin(\beta_n\theta) \tag{16}$$

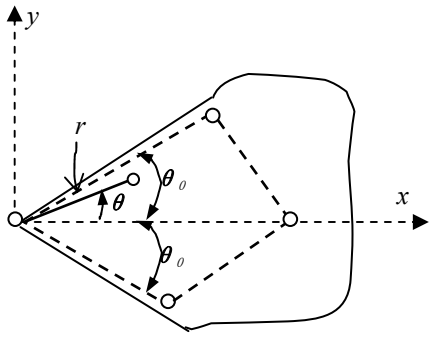

Fig. 3 a singular corner element considering an infinite wedge

where λ_n and β_n are two sets of constants which are assumed to be greater than zero. Differentiating the solution (16) and substituting it into Eqn (15) yields

$$\frac{\partial w}{\partial \theta}\Big|_{\theta=\pm\theta_0} = -\sum_{n=1}^{\infty}\lambda_n(a_n r^{\lambda_n} + b_n r^{-\lambda_n})\sin(\pm\lambda_n\theta_0) + \sum_{n=1}^{\infty}\beta_n(d_n r^{\beta_n} + e_n b^{-\beta_n})\cos(\pm\beta_n\theta_0) = 0 \tag{17}$$

Since the solution must be limited for $r=0$, we should specify

$$b_n = e_n = 0 \tag{18}$$

From Eqn (17) it can be deduced

$$\sin(\pm\lambda_n\theta_0) = 0, \quad \cos(\pm\beta_n\theta_0) = 0 \tag{19}$$

which lead to

$$\lambda_n\theta_0 = n\pi \qquad (n=1,2,3,\ldots) \tag{20}$$

$$2\beta_n\theta_0 = n\pi \qquad (n=1,3,5,\ldots) \tag{21}$$

Thus, the final form of the solution when $\theta_0 = \pi$ is

$$w(r,\theta) = a_0 + \sum_{n=1}^{\infty} a_n r^n \cos(n\theta) + \sum_{n=1,3,5}^{\infty} d_n r^{\frac{n}{2}} \sin(\frac{n}{2}\theta) \tag{22}$$

With solution (22), the internal function defined in Eqn (9) can be taken as

$$N_{2n-1} = r^n\cos(n\theta), \quad N_{2n} = r^{\frac{(2n-1)}{2}}\sin(\frac{(2n-1)}{2}\theta). \quad (n=1,2,3,\ldots) \tag{23}$$

It is obvious that the displacement function (22) include the term proportional to $r^{1/2}$, whose derivative is singular at the crack tip.

MODIFIED VARIATIONAL PRINCIPLE AND ELEMENT MATRIX

According to modified variational principle[23], the variational functional of mode III elastic fracture problem can be written as:

$$\Pi_e = \frac{1}{2}\iint_{\Omega}(q_1^2 + q_2^2)d\Omega - \int_{\Gamma_{ew}} q_n \overline{w} ds + \int_{\Gamma_{eq}} (\overline{q}_n - q_n)\tilde{w} ds - \sum \int_{\Gamma_{eI}} q_n \tilde{w} ds \tag{24}$$

where $q_1 = G\frac{\partial w}{\partial x}$, $q_2 = G\frac{\partial w}{\partial y}$.

The element matrix can be generated by the minimization of functional (24). Noting that the interpolation function $\mathbf{N}_e$ in Eqn(9) satisfies the governing equation $\nabla^2 w = 0$, we have, according to divergence theorem

$$\iint_{\Omega}(q_1^2 + q_2^2)d\Omega = \int_{\Gamma} q_n w ds - \iint_{\Omega} w(\nabla^2 w)d\Omega \tag{25}$$

Eqn (24) can thus be written as

$$\Pi_e = \frac{1}{2}\int_{\Gamma_e} q_n w ds - \int_{\Gamma_{ew}} q_n \overline{w} ds + \int_{\Gamma_{eq}} (\overline{q}_n - q_n)\tilde{w} ds - \sum \int_{\Gamma_{eI}} q_n \tilde{w} ds \tag{26}$$

Substituting expressions (9) and (12) into Eqn(26) and noting that $q_n = G\partial w / \partial n = G\mathbf{Tc}$, it gives

$$\begin{aligned}\Pi_e &= \frac{1}{2}\mathbf{c}^T(\int_{\Gamma_e}\mathbf{T}^T\mathbf{N}ds)\mathbf{c} - \mathbf{c}^T(\int_{\Gamma_{ew}}\mathbf{T}^T\overline{w}ds) + (\frac{1}{G}\int_{\Gamma_{eq}}\overline{q}_n\tilde{\mathbf{N}}ds)\mathbf{d} - \mathbf{c}^T(\int_{\Gamma_{eq}}\mathbf{T}^T\tilde{\mathbf{N}}ds - \int_{\Gamma_{eI}}\mathbf{T}^T\tilde{\mathbf{N}}ds)\mathbf{d} \\ &= -\frac{1}{2}\mathbf{c}^T\mathbf{H}\mathbf{c} + \mathbf{c}^T\mathbf{s}\mathbf{d} + \mathbf{c}^T\mathbf{r}_1 + \mathbf{d}^T\mathbf{r}_2 + f(x,y)\end{aligned} \tag{27}$$

where $f(x,y)$ does not contain parameters $\mathbf{c}$ and $\mathbf{d}$, and

$$\mathbf{H} = -\int_{\Gamma_e}\mathbf{T}^T\mathbf{N}ds \qquad \mathbf{s} = -\int_{\Gamma_{eq}}\mathbf{T}^T\tilde{\mathbf{N}}ds - \int_{\Gamma_{eI}}\mathbf{T}^T\tilde{\mathbf{N}}ds \tag{28}$$

$$\mathbf{r}_1 = -\int_{\Gamma_{ew}}\mathbf{T}^T\overline{w}ds \qquad \mathbf{r}_2 = \frac{1}{G}\int_{\Gamma_{eq}}\tilde{\mathbf{N}}^T\overline{q}_n ds \tag{29}$$

To enforce inter-element continuity on the common element boundary, the unknown vector *c* should be expressed in terms of nodal DOF **d**. An optional relationship between **c** and **d** in the sense of variation can be obtained from

$$\frac{\partial \Pi_e}{\partial \mathbf{c}^T} = -\mathbf{H}\mathbf{c} + \mathbf{s}\mathbf{d} + \mathbf{r}_1 = 0 \Rightarrow \mathbf{c} = \mathbf{B}\mathbf{d} + \mathbf{g} \tag{30}$$

where

$$\mathbf{B} = \mathbf{H}^{-1}\mathbf{s}, \qquad \mathbf{g} = \mathbf{H}^{-1}\mathbf{r}_1 \tag{31}$$

Substituting the expression (30) into Eqn (28), produces

$$\Pi_e = -\frac{1}{2}\mathbf{g}^T\mathbf{H}\mathbf{B}\mathbf{d} - \frac{1}{2}\mathbf{d}^T\mathbf{B}^T\mathbf{H}\mathbf{g} - \frac{1}{2}\mathbf{d}^T\mathbf{B}^T\mathbf{H}\mathbf{B}\mathbf{d} + \mathbf{g}^T\mathbf{s}\mathbf{d} + \mathbf{d}^T\mathbf{B}^T\mathbf{s}\mathbf{d} + \mathbf{d}^T\mathbf{B}^T\mathbf{r}_1 + \mathbf{d}^T\mathbf{r}_2 \tag{32}$$

noting the expressions (31) and using $\mathbf{s} = \mathbf{H}\mathbf{B}$ and $\mathbf{r}_1 = \mathbf{H}\mathbf{g}$, we obtain

$$\Pi_e = \frac{1}{2}\mathbf{d}^T\mathbf{B}^T\mathbf{H}\mathbf{B}\mathbf{d} + \mathbf{d}^T(\mathbf{B}^T\mathbf{H}\mathbf{g} + \mathbf{r}_2) \tag{33}$$

Therefore, the element stiffness matrix equation can be obtained by taking the vanishing variation of the functional Π_e as

$$\frac{\partial \Pi_e}{\partial \mathbf{d}^T} = 0 \qquad \Rightarrow \qquad \mathbf{Kd} = \mathbf{P} \tag{34}$$

where $\mathbf{K} = \mathbf{B}^T\mathbf{HB}$ and $\mathbf{P} = -\mathbf{B}^T\mathbf{Hg} - \mathbf{r}_2$ are, respectively, the element stiffness matrix and the equivalent nodal flow vector, the expressions of **H, s**, $\mathbf{r}_1$, $\mathbf{r}_2$ can be obtained by integrating along the corresponding boundaries of the element.

AUXILIARY FUNCTION SATISFYING SINGULAR PROPERTIES NEAR CRACK TIPS

Special purpose functions (22) is constructed by satisfying both the Laplace Eqn (1) and the free-traction boundary condition on crack faces. However, the function does not accurately meet the singular properties near crack tips because of

$$\frac{\partial w}{\partial \theta} \neq 0 \qquad (\text{for } \theta = \pm\theta_0 \text{ and } y = 0, x = 0) \tag{35}$$

and the boundary conditions near the crack tip may vary from $y = 0, x > 0$ to $y = 0, x < 0$. Due to the stress intensity factor obtained by considering the special stress behaviour around the crack tip $y = 0, x = 0$ only, so it demands an exact function to satisfy the feature near crack tip point. In fact, there are not contributions of the term $\partial w / \partial \theta$ to the stiffness matrix and equivalent nodal flow vector (Eqn (34)) in crack elements due to Eqn (15) whereas exact function can directly do within crack elements. It is important for us to simulate an exact function near crack tip $y = 0, x = 0$.

According to the particular boundary conditions (35), the displacements and stress prescribed along both sides around $y = 0, x = 0$ should be completely equal within a very small region around crack tip, called micro size. The displacements and stress along $y = 0, x < 0$ can be deduced by analysing displacement behaviour on another side, and there are several approximate approaches have been adopted to satisfy the upper character before (Portela [31], Sabino et al [28], Qin [32]).

From this point of view, the paper presents an approximate approach----auxiliary function approach in which the displacements satisfy singular properties near crack tips. In this approach, the displacements and stress along the left micro size of $y = 0, x = 0$ is expressed in terms of some analytical functions which can simulate the characters along the right micro size. Meanwhile, the auxiliary functions used should also approximately agreed with Laplace Eqn(1) and the boundary conditions around the region of left micro size $y = 0, x = 0$. In fact, these kinds of auxiliary functions can be simulated easily as well.

There two major advantages in using the auxiliary function approach. One is that the accuracy of results near crack tips can be improved when the computation involves the region far from crack tips; another is that the same results can be achieved using different auxiliary functions. This feature can be applied to check the correctness of the outcomes as well. In general, when using stiffness matrix and equivalent nodal flow vector defined in Eqn (34) to study singular intensity character the use of auxiliary function in crack elements is promising to improve computing accuracy.

SINGULAR INTENSITY FACTOR FOR MODE III ELASTIC PROBLEM

Generally, stress intensity factors(SIF) can be evaluated by analysing stress and displacement fields near crack-tips using various numerical methods such as conventional FEM and boundary element method. These procedures are usually complicated and time-consuming. In contrast, SIF can be easily estimated by using the special purpose function discussed in this paper. Typically, the stress intensity factors K_{III} can be straightforwardly evaluated from the results of unknown vector **c**. To show this, consider that stress singularity near crack tip is of $r^{-1/2}$ type:

$$\sigma_{23} = \frac{K_{III}}{\sqrt{2\pi r}} \cos\frac{\theta}{2} \tag{36}$$

and when $\theta = 0$

$$K_{III} = \lim_{r\to 0} \sqrt{2\pi r}\,\sigma_{23} \tag{37}$$

substituting Eqns (4) and (9) into Eqn (36), we have

$$K_{III} = \lim_{r\to 0} \sqrt{2\pi r}\, G \frac{\partial \mathbf{N}}{\partial y}\mathbf{c} \tag{38}$$

When the cracks tip is located at the origin of the coordinate by using a polar coordinate (see Fig.3), Eqn (38) can be written as

$$K_{III} = \lim_{r\to 0} \sqrt{2\pi r}\, G \frac{1}{r}\left(\frac{\partial N_1}{\partial \theta} c_1 + \frac{\partial N_2}{\partial \theta} c_2 + \frac{\partial N_3}{\partial \theta} c_3 + \frac{\partial N_4}{\partial \theta} c_4\right) \tag{39}$$

For example, when m=4, the T-complete system solutions are:

$$\frac{\partial N_1}{\partial \theta} = -r\sin\theta\,,\ \frac{\partial N_2}{\partial \theta} = \frac{1}{2} r^{\frac{1}{2}} \cos\frac{\theta}{2},\ \frac{\partial N_3}{\partial \theta} = -2r^2 \sin 2\theta\,,\ \frac{\partial N_4}{\partial \theta} = \frac{3}{2} r^{\frac{3}{2}} \cos\frac{3}{2}\theta \tag{40}$$

substituting (40)into Eqn(39), it can be obtained the expression of stress singular factor

$$K_{III} = \frac{\sqrt{2\pi}}{2} G c_2 \tag{41}$$

In general, when $\theta_0 \neq \pi$, the singularity becomes the type of $r^{\lambda-1}$, where $\lambda = 1 - \frac{\pi}{2\theta_0}$. In this case the general expression of stress intensity factors are formally defined as

$$K_{III} = \lim_{r\to 0}\left[\frac{(2\pi)^{1/2}}{r^{1-\lambda}} \sigma_{23}(r,0)\right] \tag{42}$$

it can finally be written as:

$$K_{III} = \sqrt{2\pi} G c_2 \frac{\pi}{2\theta_0} \tag{43}$$

NUMERICAL ASSESSMENT

As numerical illustrations of the proposed element formulation, Fig.4 shows a rectangular plate with a side mode III crack. Owing to the symmetry of the problem, the element meshing shown in Fig. 4 models only half of the plate. The boundary conditions of the problem are

$y = 0, x < 0$, $\sigma_{23} = 0$;

$y = 0$, $x \geq 0$, $u = 0$;

$-h \leq y \leq h, x = -a$ and $x = (b-a)$, $\sigma_{31} = 0$;

$y = \pm h, -a \leq x \leq (b-a)$, $\sigma_{23} = \pm q$ (44)

In the analysis, the 4-node quadrilateral elements are used for modelling regular element and 5-node and 7-node elements are used in special crack elements. The ratio *a*/*b* is taken to be 0.5 in our analysis. In the

Gauss integration, the number of Gauss points can be determined by the general solution system. In the calculation a local coordinate system is adopted to avoid developing ill-conditioned matrix and the singular value decomposition solver is serviced in the computation.

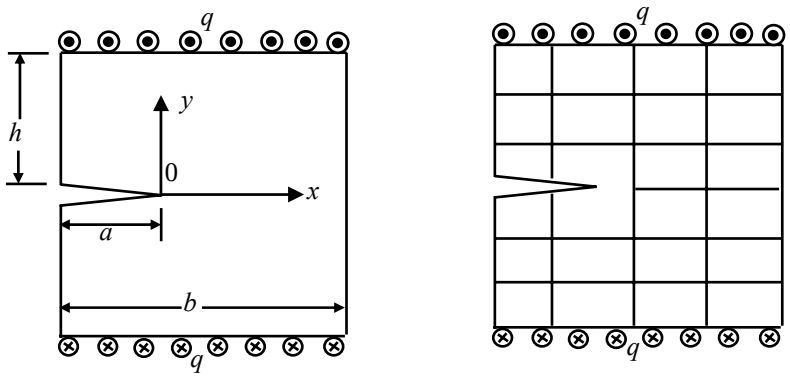

Fig.4 Mode III crack problem and its meshing

For the rank condition[16], the number of T-functions should be satisfy when $m \geq 3$ for regular elements and $m \geq 6$ for special purpose elements. The auxiliary functions used in the calculation are:

$$q = \frac{\zeta}{b^a}(r^a - b^a)\cos\theta \qquad a < 1.0 \tag{45}$$

$$q = \frac{\zeta}{b^a}(b - r)^a \cos\theta \qquad a \geq 1.0 \tag{46}$$

where ζ is a constant for the different situations of auxiliary functions. The following is the discussion of the computing results:

Table 1 shows the results of stress intensity factors versus the number of special T-functions for the side mode III crack problem (Fig.4) when $a/b = 0.5$. It can be seen that the ratio of K_{HT}/K_c (K_{HT} is the SIF by computing and K_c can refer to [32-33]) gradually decreases when the number of special T-functions increases and converge to 1.144 when the number of special T-functions $\geq$ 8.

Table 1 Stress Intensity Factors Versus the Number of Special T-Functions ($a/b = 0.5$) K_{HT}/K_c (K_{HT} is the SIF by Computing and K_c can Refer to [32-33])

Number of special T-functions	K_{HT}/K_c
4	1.279
6	1.156
8	1.146
10	1.144
12	1.144

The results of singular intensity factor K_{HT}/K_c versus the number of crack elements are listed in Table 2. It is found from Table 2 that the ratio of K_{HT}/K_c slightly decreases along with an increase in the number of crack elements. It also converge to 1.144 when the number of crack elements $\geq$ 4.

Table 2 Stress Intensity Factors Versus the Number of Crack Elements $(a/b=0.5)\,K_{HT}/K_c$

Number of crack elements	K_{HT}/K_c
1	1.161
2	1.149
3	1.145
4	1.144
5	1.143

Table 3 lists the results of singular intensity factors versus two types of auxiliary functions. It can be seen that the two auxiliary functions gives almost the same results of the ratio of K_{HT}/K_c and achieve convergence when the number of crack elements $\geq$ 15 for Eqn (46) and the number of crack elements $\geq$ 6 for Eqn (45).

Table 3 Stress Intensity Factors Versus Two Types of Auxiliary Functions $(a/b=0.5)\,K_{HT}/K_c$

Auxiliary function near crack tips	K_{HT}/K_c
Eqn(45)(number of crack elements=15)	1.146
Eqn(46))(number of crack elements=6)	1.143

To further assess the performance of the proposed element model, the displacement and stress fields in some particular elements and nodes are analysed, particularly at the nodes between the crack element and regular element. When using the auxiliary functions, the order of accuracy of displacement and stress in the left and the right micro size around *x=0, y=0* is about 10^{-3} to 10^{-4} , while the corresponding order of accuracy for those points far from *x=0, y=0* is about 10^{-2} to 10^{-3} only. As for the regular elements, the precision of 10^{-6} to 10^{-8} can be obtained in this example, which is much lower than that of crack elements. It also found that the order of accuracy is much higher than those obtained from conventional finite element model.

CONCLUSION

Applications of Trefftz finite element method to mode III elastic fracture problems are presented based on special purpose functions for singular corner, auxiliary functions, and a modified variational principle in the paper. Trefftz finite element formulation including special purpose elements and auxiliary functions within the microsize of crack tips are discussed in details. The performance of special proposed element model is assessed by a numerical example of a rectangular plate with a side mode III crack. The study showed that stress intensity factors by the number of crack elements and the number of special T-functions. The value of K/K_c decreases along with an increase either the number of crack element or the number of special T-functions, but it converge to a certain value. It is also found that SIF can converge to the same value even using different auxiliary function, which provides a means for us to check the correctness of the results. The proposed Trefftz finite element approach is demonstrated to be ideally suited for the analysis of the fracture problem.

REFERENCES

[1] Jirousek, J. & Leon, N., *A powerful finite element for plate bending*, Comp. Meth. Appl. Mech. Eng., 12, (1977), 77-96.

[2] Jirousek, J. & Venkatesh, *A. Hybrid-Trefftz plane elasticity elements with p-method capabilities*, Int. J. Numer. Meth. Eng., 35, (1992), 1443-1472.

[3] Piltner, R., *Special finite elements with holes and internal cracks*, Int. J. Numer. Meth. Eng., 21, (1985), 1471-1485.

[4] Jirousek, J. & Guex, L., *The hybrid-Trefftz finite element model and its application to plate bending*, Int. J. Numer. Meth. Eng., 23, (1986), 651-693.

[5] Qin, Q.H., *Hybrid Trefftz finite element approach for plate bending on an elastic foundation*, Appl. Mathe. Modelling, 18, (1994), 334-339.

[6] Jin, F.S. & Qin, Q.H., *A variational principle and hybrid Trefftz finite element for the analysis of Reissner plates*, Compu. & Struc, 56, (1995), 697-701.

[7] Jirousek, J., Wroblewski, A., Qin, Q.H. & He, X.Q., *A family of quadrilateral hybrid Trefftz p-element for thick plate analysis*, Comp. Meth. Appl. Mech. Eng., 127, (1995), 315-344.

[8] Qin, Q.H., *Hybrid Trefftz finite element method for Reissner plates on an elastic foundation*, Comp. Meth. Appl. Mech. Eng., 122, (1995), 379-392.

[9] Piltner, R., *A quadrilateral hybrid-Trefftz plate bending element for the inclusion of warping based on a three-dimensional plate formulation*, Int. J. Numer. Meth. Eng., 33, (1992), 387-408.

[10] Piltner, R., *On the representation of three-dimensional elasticity solutions with the aid of complex value functions*, J. Elasticity, 22, (1989), 45-55.

[11] Stein E. and Peters K., *A new boundary-type finite element for 2D and 3D elastic solids*, The Finite Element Method in the 1990s, a book dedicated to O.C. Zienkiewicz, Eds. E. Onate, J. Periaux & A. Samuelson, Springer: Berlin, 35-48, (1991).

[12] Wroblewski, A., Zielinski, A.P. & Jirousek, J., *Hybrid-Trefftz p-element for 3-D axisymmetric problems of elasticity*, Numerical methods in Engineering'92, Proc. First Europ. Conf. On Numer. Meth. in Eng., eds. C. Hirsch, O.C. Zienkiewicz & E. Onãte, Brussel, Elsevier, pp.803-810, (1992).

[13] Jirousek, J. & Stojek, M., *Numerical assessment of a new T-element approach*, Compu. & Struc., 57, (1995), 367-378.

[14] Zielinski, A.P. & Zienkiewicz, O.C., *Generalized finite element analysis with T-complete boundary solution functions*, Int. J. Numer. Meth. Eng., 21, (1985), 509-528.

[15] Vörös, G.M. & Jirousek, J., *Application of the hybrid-Trefftz finite element model to thin shell analysis*, Proc. Europ. Conf. on new Advances in Comp. Struc. Mech., eds. P. Ladeveze & O.C. Zienkiewicz, Giens, France, pp.547-554, Elsevier, (1991).

[16] Qin, Q.H., *The Trefftz Finite and Boundary Element Method*, WIT Press, Southampton, UK, (2000).

[17] Markiewicz, M. & Mahrenholtz, O., *Combined time-stepping and Trefftz approach for nonlinear wave-structure interaction*, Computer Assisted Mechanics and Engineering Sciences, 4, (1997), 567-586.

[18] Qin, Q.H., *Transient plate bending analysis by hybrid Trefftz element approach*, Communi. Numer. Meth. Eng., 12, (1996), 609-616.

[19] Jirousek, J. & Qin, Q.H., *Application of Hybrid-Trefftz element approach to transient heat conduction analysis*, Compu. & Struc., 58, (1996), 195-201.

[20] Qin, Q.H., *Postbuckling analysis of thin plates by a hybrid Trefftz finite element method*, Comp. Meth. Appl. Mech. Eng., 128, (1995), 123-136.

[21] Qin, Q.H., *Nonlinear analysis of thick plates by HT FE approach*, Compu. & Struc., 61, (1996), 271-281.

[22] Qin, Q.H., *Postbuckling analysis of thin plates on an elastic foundation by HT FE approach*, Appl. Math. Modelling, 21, (1997), 547-556.

[23] Qin, Q.H. & Diao S., *Nonlinear analysis of thick plates on an elastic foundation by HT FE with p-extension capabilities*, Int. J. Solids Structures, 33, (1996), 4583-4604.

[24] Freitas, J.A.T. & Wang, Z.M., *Hybrid-Trefftz stress elements for elastoplasticity*, Int. J. Numer. Meth. Eng., 43, (1998), 655-683.

[25] Zielinski, A.P., *Trefftz method: elastic and elastoplastic problems*, Comp. Meth. Appl. Mech. Eng., 69, (1988), 185-204.

[26] Jirousek, J. & Teodorescu, P., *Large finite elements method for the solution of problems in the theory of elasticity*, Compu. & Struct., 15, (1982), 575-587.

[27] Venkatesh, A. & Jirousek, J., *Accurate representation of local effect due to concentrated and discontinuous loads in hybrid-Trefftz plate bending elements*, Compu. & Struct., 57, (1995), 863-870.

[28] Sabino, J., Portela A. & Castro P.M.S.T. de, *Trefftz boundary element method applied to fracture mechanics*, Eng. Frac. Mech., 64, (1999), 67-86.

[29] Freitas, J.A.T. & Ji, Z.Y., *Hybrid-Trefftz equilibrium model for crack problems*, Int. J. Numer. Meth. Eng., 39, (1996), 569-584.

[30] Horgan, C.O. & Miller, K.L., *Antiplane shear deformations for homogeneous and in homogeneous anisotropic linearly elastic solids*, J. Appl. Mech., 61, (1994), 23-29.

[31] Portela, A., Aliabadi, M.H. and Rooke, D.P., *The dual boundary element method: Effective implementation for crack problems*, *Int. J.* Numer. Methods Eng., 33, (1992), 1269-1287.

[32] Qin, Q.H., *Solving anti-plane problems of piezoelectric materials by the Trefftzfinite element approach*, Computational Mechanics, 31, (2003), 461-468.

[33] Zhang, X. S., *Thegeneral solution of an edge crack off the center line of a rectangular sheet for Mode III*, Eng. Fract. Mech., 31, (1988), 847-855.

Trefftz-type elements, or T-elements, are finite elements the internal field of which fulfils the governing differential equations of the problem a priori whereas the interelement continuity and the boundary conditions are enforced in an integral weighted residual sense or pointwise. Although the key ideas of such elements can be traced back to Jirousek and Leon in 1977, the T-element approach has received serious attention only for the past ten years. The T-element approach makes it possible to generate highly accurate h- or p-elements exhibiting many important advantages over their more conv Finite Element Analysis, or FEA, is the process at the core of mechanical engineering and one of the key principles for simulation realm.Â The history of finite element analysis. The beginnings of FEA date back to the famous mathematician Euler, in the 16th century. However, a more rigid definition of "FEA" traces the first mention of the method back to the works of Schellbach in 1851. Finite Element Analysis was a process developed for engineers by engineers as a means to address structural mechanics problems in civil engineering and in aerospace. Source: Craig Bonsignore/Flickr. This practical intention of the methodology meant that from the beginning, these methods were designed as more than just mathematical theory. Fundamentals of Finite Element Analysis: Linear Finite Element Analysis. 729 PagesÂ·2018Â·28.5 MBÂ·33,986 DownloadsÂ·New! of the method for linear problems. A general procedure is presented for the finite element Structural Analysis with the Finite Element Method. Linear Statics: Volume 1: Basis and Solids (Lecture Notes on Numerical Methods in Engineering and Sciences) (v. 1). 495 PagesÂ·2009Â·25.23 MBÂ·12,290 DownloadsÂ·New! STRUCTURAL ANALYSIS WITH THE FINITE ELEMENT METHOD Linear Statics Volume 1 : T The Finite Element Method: Linear Static and Dynamic Finite Element Analysis. 672 PagesÂ·20 Some books devoted exclusively to ï¬nite element analysis include some examples about modeling composites but fall quite short of dealing with the actual analysis and design issues of composite materials and com- posite structures. This textbook includes an explanation of the concepts involved in the detailed analysis of composites, a sound explanation of the mechanics needed to translate those concepts into a mathematical representation of the physical reality, and a detailed explanation of the solution of the resulting boundary value problems by using commercial Finite Element Analysis softwa...Â This textbook bridges the gap between powerful ï¬nite element tools and practical problems in structural analysis of composites. In mathematics, the Trefftz method is a method for the numerical solution of partial differential equations named after the German mathematician Erich Trefftz(de) (1888â€“1937). It falls within the class of finite element methods. The hybrid Trefftz finite-element method has been considerably advanced since its introduction about 30 years ago. The conventional method of finite element analysis involves converting the differential equation that governs the problem into a variational functional from which